Photocatalytic activity of a new composite material of Fe (III) oxide nanoparticles wrapped by a matrix of polymeric carbon nitride and amorphous carbon

Roberto C. Dante[1,*], Francisco M. Sánchez-Arévalo[2], Lazaro Huerta[2], Florinella Muñoz-Bisesti[3], Diana Marquez[3], Pablo Martín-Ramos[4], Luis Lartundo-Rojas[5], Pedro Chamorro-Posada[6], Omar Solorza-Feria[7]

[1]2Dto3D S.r.l.s., Via Revalanca 5 (San Firmino), 12036 Revello (CN), Italy.

[2]Departamento de reología y mecánica de materiales, Instituto de Investigaciones en Materiales (IIM), Universidad Nacional Autónoma de México (UNAM), Apdo. Postal 70--360, Cd. Universitaria, Mexico City 04510, Mexico.

[3]Departamento de Ciencias Nucleares, Facultad de Ingeniería Química y Agroindustria, Escuela Politécnica Nacional (EPN), Ladrón de Guevara E11-253, Quito, Ecuador.

[4]EPS, Instituto Universitario de Ciencias Ambientales de Aragón (IUCA), Universidad de Zaragoza, Carretera de Cuarte s/n, 22071, Huesca, Spain.

[5]Instituto Politécnico Nacional, Centro de Nanociencias y Micro y Nanotecnologías de Nanociencias, UPALM, Zacatenco, Mexico City, 07738, Mexico.

[6]Dpto. de Teoría de la Señal y Comunicaciones e IT, Universidad de Valladolid, ETSI Telecomunicación, Paseo Belén 15, 47011 Valladolid, Spain.

[7]Departamento de Química, Centro de Investigación y de Estudios Avanzados del Instituto Politécnico Nacional (CINVESTAV-IPN). Av. IPN 2508, Col. San Pedro Zacatenco, Apdo. Postal 14--740, Mexico D.F. 07360, Mexico.

[*]Corresponding author, email: rcdante@yahoo.com

Abstract

Polymeric carbon nitride was synthesized from urea and doped with Cu and Fe to act as co-catalysts. The material doped with Fe was a new composite material composed of Fe(III) oxides (acting as a co-catalyst) wrapped by the polymer layers and amorphous carbon. Furthermore, the copper doped material was described in a previous report. The photocatalytic degradation of the azo dye direct blue 1 (DB) was studied using as photocatalysts: pure carbon nitride (CN), carbon nitride doped with Cu (CN-Cu), and carbon nitride doped with Fe (CN-Fe). The catalysts were characterized by Fourier transform infrared (FTIR) spectroscopy, X-ray diffraction (XRD), by X-ray photoelectron spectroscopy (XPS), and Brunauer–Emmett–Teller method (BET), etc. The adsorption phenomenon was studied using the Langmuir and Freundlich models. For the kinetic study, a solution of 500 mg L^{-1} of DB1 was treated with each catalyst, visible light, and H_2O_2. The dye concentration was measured by spectrophotometry at the wavelength of 565 nm, and the removal of the total organic content (TOC) was quantified. BET analysis yielded surface areas of 60.029, 20.116 and 70.662 m^2 g^{-1} for CN, CN-Cu, and CN-Fe, respectively. The kinetics of degradation were pseudo-first order, whose constants were 0.093 min $^{-1}$, 0.039 min $^{-1}$ and 0.110 min $^{-1}$ for CN, CN-Cu and CN-Fe, respectively. The total organic carbon (TOC) removal reached the highest value of 14.46% with CN-Fe.

Keywords

Photocatalyst, carbon nitride, iron oxide, nanoparticles, co-catalyst

1. Introduction

Graphitic carbon nitride (g-C_3N_4) is a mesoporous material with as a basic unit heptazine (1), which has captured the attention of the scientific community due to its optoelectronic characteristics as to its high thermal and chemical stability, its semiconductor behavior, energy storage capacity, and gas adsorption (2), etc. In fact, this compound has been tested in fuel cells, electronic sensors, and photocatalysis with promising results (3). The synthesis of this material can be carried out from many compounds containing carbon and nitrogen in the right proportion. The main processes of synthesis correspond to the polymerization of compounds such as cyanamide, dicyanamide (2), melamine, melamine cyanurate, and uric acid (4) or by pyrolysis of urea, a low cost reagent (5).

The structure of graphite carbon nitride allows it to interact with ions and polar species, so it is possible to dope this material with fluorine, boron (6), iron (7), copper (8, 9), manganese (10), nickel, or cobalt (11). The doping of carbon nitride enhances either the conversion or selectivity of the catalyst (9) by affecting its morphology, its response to visible light and its photocatalytic activity (12). Since it is sensitive to light, carbon nitride may be an alternative to the use of titanium dioxide (TiO_2) in the degradation of pollutants.
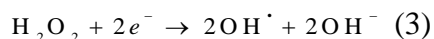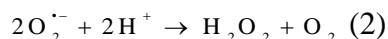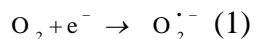
Carbon nitride presents band gap values, typical of wide band gap semiconductor materials, which makes it a potential photocatalyst for cyclic organic compounds, and effective in various reactions such as the photochemical splitting of water, selective oxidation reactions, and reactions of hydrogenation (13). Dante et al. (9) reports bandwidths of 2.90 eV for pure carbon nitride and 2.88 eV for carbon nitride doped with copper. These band gaps give to graphitic

carbon nitride a redox potential that allows it to catalyze reactions efficiently, so it is able to generate active species in the presence of visible light (14).

This catalyst has been used in the degradation reaction of dyes such as methylene blue (MB) [5], rhodamine B (RhB) [11] and methyl orange, an azo-derivate dye. On the other hand, it has been demonstrated that carbon nitride can be industrially used for the treatment of effluents (15). Azo-dyes derives from aromatic hydrocarbons, made up of benzene, toluene, naphthalene, phenol and aniline. In addition, they are the most important and widely used group of synthetic dyes in the textile, pharmaceutical and printing industries. Its use has been extended due to its stability to light and washing. Azo-derivative dyes are estimated to account for more than 50% of the annual dye production. It is presumed that approximately 2000 different azo dyes are currently used in the industry, and their worldwide production amounts to $7 \cdot 10^5$ tons. It is estimated that the 10% of the dyes used in textile dyeing do not adhere to the fibers, so they will be present in their effluents (16). Azo-dyes are difficult to degrade because their structure is chemically stable. These compounds are carcinogenic and mutagenic, thus posing a danger to aquatic and animal organisms (17). The advanced oxidation processes (AOPs) arise as an alternative to traditional treatments to make the degradation of this type of pollutants more efficient through the generation of free radicals (18). An example of AOP is heterogeneous photocatalysis, which involves light and, as a catalyst, a semiconductor material. Due to the properties mentioned above, it is feasible to employ carbon nitride as the catalyst in an AOP.

It is not possible to carry out an AOP in the absence of hydroxyl radicals, so that an oxidizing agent is necessary. Yan et al. reported that the presence of O_2 is an important factor in photo-degradation processes with carbon nitride (15). O_2 affects the formation of superoxides by direct

reduction of O_2 according to the reactions shown in equation 1. In turn, hydrogen peroxide can form the hydroxyl radicals which is very reactive. (equations 2 and 3).

$$O_2 + e^- \rightarrow O_2^{\cdot-} \quad (1)$$

$$2O_2^{\cdot-} + 2H^+ \rightarrow H_2O_2 + O_2 \quad (2)$$

$$H_2O_2 + 2e^- \rightarrow 2OH^{\cdot} + 2OH^- \quad (3)$$

The aim of the present research was to study the degradation of the blue azo-dye DB1 (whose molecular structure is shown in Figure 1 via an heterogeneous photo-catalysis utilizing hydrogen peroxide as oxidizing agent, and as photocatalysts: pure carbon nitride (CN), carbon nitride doped with copper(CN-Cu), and carbon nitride doped with iron (CN-Fe).

During the synthesis of the composite material doped with iron, Fe(III) oxides were formed, including polymeric carbon nitride, and amorphous carbon. Moreover, it is noteworthy to point out that this composite material could be used not only to photo-oxidize organic matter but even to split water. Indeed, the band gap of Fe(III) oxides could work to the half reaction of water oxidation H_2O/O_2. However, it has been reported that an optimal band gap of 2.46 eV (19) is required for water photo-oxidation without an external bias. Although the band gap of hematite, reported to be around 1.9 to 2.2 eV (depending on its crystalline status and methods of preparation), and its valence band edge are suitable for oxygen evolution, the conduction band edge of hematite is too low to generate hydrogen. Therefore, iron (III) oxides could be suitable to be coupled to polymeric carbon nitride whose band gap is between 2.4 and 3.0 eV so that to obtain an interesting co-catalyst to split water.

2. Analysis methods

2.1. Synthesis and characterization of the catalysts

The synthesis of the catalysts was carried out by pyrolysis of 30 g of urea, and 0.5 g of the respective doping salt, either copper sulfate pentahydrate ($CuSO_4 \cdot 5H_2O$) or iron sulfate heptahydrate ($FeSO_4 \cdot 7H_2O$). The reaction took place in a muffle Vulcano A-130 at 600 ºC, without air flow, with monitored heating. Firstly, the temperature was raised to reach 600 °C to pyrolize urea. The pyrolysis times, obtained in preliminary tests, were of 40, 10, and 30 minutes to synthetize pure carbon nitride (CN), doped with copper (Cu-CN) and doped with iron (Fe-CN), respectively. Once the samples reached the room temperature inside the muffle, were retired and the reaction yield was determined by gravimetry. The Fourier transform infrared (FTIR) spectra of the samples were obtained by means of a spectrometer Agilent FTIR Cary 630. The X-ray diffraction patterns of the catalysts were carried out with a Rigaku ULTIMA-IV Bragg-Brentano powder diffractometer with Cu Kα radiation. The atomic absorption analyses to determine the metal contents were performed by means of a Perkin Elmer A-Analyst 300 equipment. UV-Vis diffuse reflectance spectra were measured using a Perkin Elmer Lambda 35 UV-Vis spectrophotometer. The study by transmission electron microscopy (TEM) was carried out with a JEM-ARM200 F. Complete XRD, Uv-vis, XPS and TEM results are presented in the Supplementary Information. The description of these research methods were reported in the Supplementary Information. The characterization of the copper doped material is not reported because was already reported by Dante et al. in a previous research report (9). The surface area Brunauer-Emmett-Teller (BET) of the catalysts was determined by means of the Quantachrome equipment, NovaWin v11.0,through adsorption of the N_2.

2.2. Rating of the photo-catalytic activity of the catalyst

Solutions with concentration of the blue dye DB1 of 500 mg/L were used for the experiments, at 20 °C and pH = 7. The concentration of the colorant in every sample was determined by spectrophotometry UV-VIS at 565 nm with a spectrophotometer Hitachi model U-1 900.

2.2.1. Adsorption equilibrium

In order to determine the time to reach the adsorption equilibrium 20 mL of colored solution and 20 mg of CN were placed in different Petri boxes. After 5, 10, 20, 30, 40, 50, 60, 120, and 180 minutes, and simultaneously the samples were centrifuged for 3 minutes at 1200 rpm and the concentration of the supernatant was quantified (20). The process was repeated for CN-Cu and CN-Fe.

2.2.2. Isotherms of adsorption

Aliquots of 20 mL of the dye solution were placed in Petri boxes and 5, 10, 14, 17, and 20 mg of the catalyst were added to different boxes. Once spent the time to reach the adsorption equilibrium, determined in the previous tests, the samples were centrifuged for 3 minutes at 1200 rpm. The dye concentration was measured in the supernatant by UV-Vis spectrophotometry. The adsorbed mass for each test was calculated according to equation 4.

$$q_e = \frac{(C_0 - C_f)V}{m}. \ (4)$$

The models of Langmuir and Freundlich were used to determine the adsorption mechanism, according to equations 5 and 6.

$$\frac{C_e}{q_e} = \frac{1}{k_L q_{max}} + \frac{1}{q_{max}} C_e; \ (5)$$

$$Ln q_e = \frac{1}{n} \ln C_e + \ln k_F. \ (6)$$

C_o and C_f are the initial and final concentration of the dye, respectively. V is the volume of the solution, m is the mass of the catalyst, and q_e is the adsorbed mass of the dye per unit mass of the catalyst. For the models of Langmuir and Freundlich, C_e is the solution concentration in equilibrium, q_{max} is the maximum quantity of dye adsorbed by each suspension, k_L is the equilibrium constant of the Langmuir's model and the constants of the Freundlich's model are k_F and n (21). These tests have been carried out with the three synthetized catalysts.

2.2.3. Photocatalytic activity

An aliquot of 20 mL of DB1 solution and 20 mg of catalyst were placed in a Petri box. Once reached the adsorption equilibrium, the necessary quantity of dye was added (using a very concentrated solution) to obtain a solution with a dye concentration of 500 mg/L. This ensured the same initial concentration of the dye, in the samples with different catalysts. An aliquot of 1 mL of a solution at 30 V% H_2O_2 was added as an oxidizing agent and the light of a 35 W Xe lamp (positioned at a distance of 3 cm from the base of the Petri box) was impinged on the mixture during different times under constant stirring at 300 rpm and 20 ° C. Temperature was kept constant by means of a bath with water cooling. The samples were centrifuged for 3 min at 1200 rpm. The degradation kinetic parameters of the blue dye DB1 were determined for each catalyst.

Under the conditions described above, the kinetics of degradation of the dye in the absence of catalyst, i.e. using only the oxidizing agent, were also evaluated. The percentage of removal of the total organic carbon (TOC) at the end of the degradation of the dye, with each of the catalysts, was also assessed, with respect to the DB1 solution of 500 mg L^{-1}, by means of an automated Shimadzu TOC – 5000 A.

2.3. Reuse of catalysts

The efficiency of each of the catalysts in the degradation of the DB1 blue dye was evaluated repeating three times the photocatalytic tests with the same sample.

The exposure time to the Xe lamp varied for each catalyst, and corresponded to the point at which a dye degradation larger than the 99% was achieved. Then, the sample was centrifuged and the residual amount of dye was quantified. This involved a treatment cycle. Afterwards, the solution was completely evaporated at 30 °C and the process was repeated until the third reuse of the catalyst (5).

3. Results and discussion

3.1. Synthesis and characterization of the catalysts

As a result of the synthesis of the catalysts, a powder with characteristics similar to those reported by (10) was obtained. CN was a pale yellow powder, CN-Cu obtained showed a yellow-greenish colour, while CN-Fe was brown-reddish.

For the synthesis reaction of the catalysts from urea pyrolysis, the average mass yields obtained were of 2.38% for pure carbon nitride, 5.88% for copper doped carbon nitride, and 2.10% for iron- doped carbon nitride. Liu et al. (5) reported yields of 4%, for the synthesis reaction of pure carbon nitride from urea.

The effective polymeric carbon nitride synthesis was confirmed by the FTIR spectrum of the synthesized catalysts (see Figure 2).

The polymeric carbon nitride characteristic bands were reported by Lin et al. (14) and Dante et al. (9). The interaction of the N-H bond generates the bands between $3250 \, cm^{-1}$ and

3083 cm^{-1}. The peak at 1409 cm^{-1} corresponds to the CN stretching of the tertiary nitrogen atoms found in the middle of the carbon nitride structure, whereas the peak at 1227 cm^{-1} corresponds to the vibrational modes of secondary nitrogens, units C-NH-C. These two peaks determine the process of formation of C_3N_4. The bands occurring at 1310 cm^{-1} and 1627 cm^{-1} are associated with the stretching of C (sp^2) -N and C (sp^2) = N respectively. The band at 1558 cm^{-1} can be associated to NH$_2$ scissoring. The band at 891 cm^{-1} occurs due to deformation of the polymer skeleton. The peak at 805 cm^{-1} is associated with the deformation of the tri-*s*-triazine ring (14,9). The IR spectra of CN-Cu and CN-Fe did not show any evident effect of either copper or iron on the characteristic bands, and are similar to the spectrum of CN (9).

The atomic absorption tests were carried out in order to determine the real amount of metals doping the polymeric carbon nitride. CN-Cu contained the $5.85 \cdot 10^{-3}$ g Cu g^{-1} of catalyst, and CN-Fe presented 0.37 g Fe g^{-1} catalyst. Although the mass amount of doping salt during the synthesis of these two catalysts was the same, it was evidenced that in the case of CN-Fe, large amount of the metal were incorporated and probably this was the cause of the lowering of the crystallinity degree. Moreover, it was found that iron was oxidized as determined by XPS (Supplementary Information), and amorphous carbon is present too in a considerable amount (not detectable by FTIR). It was possible to detect nanoparticles of iron oxide by TEM (see Figure 3), which are completely wrapped by the composite matrix. The iron oxide particles are FeO(OH) of Goethite phase, as determined by the measured interplanar distances (Supplementary Information). Both materials are semiconductors so that they can work together

increasing the whole efficiency. The optical band gap of the Fe (III) oxide was 1.97 eV and that of polymeric carbon nitride 2.67 eV (Supplementary Information).

Moreover, XPS of C1s (shown in the Supplementary Information) showed the presence of a considerable amount of amorphous carbon (apart the polymeric carbon nitride), not present in the copper doped material. The formation of this type of carbon makes this material much more complex, and possibly useful also to electrodes. In summary, this material can be considered a composite of several phases, including amorphous carbon, polymeric carbon nitride, which wraps the Fe(III) oxide nanoparticles.

The results of the BET analysis indicated that the surface area of CN was 60.03 $m^2 g^{-1}$, 20.12 $m^2 g^{-1}$ for CN-Cu, and 70.66 $m^2 g^{-1}$ for CN-Fe.

Sridharan et al. (11) reported a surface area of 27.7 $m^2 g^{-1}$ for pure carbon nitride and 42.9 $m^2 g^{-1}$ for carbon nitride doped with iron. Han et al. (8), reported a surface area of 30.1 $m^2 g^{-1}$ for copper doped nitride. In the present study, it was possible to synthesize pure carbon nitride and iron-doped nitride with larger surface areas than those reported in other research reports. However, it was not possible to improve the area of copper-doped carbon nitride by this method of synthesis.

The differences in the surface areas, compared to that reported by other authors, could then be due to the different synthesis methods (especially time and the utmost temperature), which can either increase or decrease the porosity.

3.2. Evaluation of photocatalytic activity of catalysts

3.2.1. Adsorption equilibrium

The variation of the solution concentration (initial value 500 mg L^{-1}, 20 mL) of the blue dye B1 was determined with respect to the time taken for the solution to reach the adsorption equilibrium. The results are shown in Table 1. In the case of CN, a 11.24% removal was achieved by adsorption after 10 min. For CN-Cu, the adsorption achieved a removal of 7.07%. This happened at 120 min. Finally, for CN-Fe, the 18.47% of the DB1 blue dye was removed after 120 min.

Adsorption is directly related to the adsorbent mass, which means that the higher the mass of the catalyst, the dye concentration in the solution, after adsorption, will be lower (22). The adsorbed mass corresponds to the mass of adsorbed dye (mg) per gram of catalyst, and was 56.318, 35.49 and 92.56 mg of dye per g of catalyst, for CN, for CN-Cu, and CN-Fe, respectively. Lee et al. (23) reported that the amine functional groups present in the carbon nitride structure could improve the performance of said catalyst as an adsorbent. NH and NH$_2$ groups within the structure of carbon nitride are basic active sites present on the surface which dye molecules (in this case DB1) with sulfonic acidic groups (R-SO$_3$H) adhere to (24).

3.2.2. Adsorption isotherms

For the construction of adsorption isotherms, the concentration of the initial solution was kept constant and the amount of catalyst varied. Table 1 shows the parameters of the Langmuir and Freundlich models calculated for the adsorption of DB1 with each of the synthesized catalysts. It can be seen that the three catalysts fitted the Freundlich model, suggesting that the adsorption phenomenon occurred in multiple layers. The Freundlich equation usually adjusts to aqueous

ACCEPTED MANUSCRIPT

solution adsorption processes. The parameters of the Freundlich isotherm, k_F and n, are system-specific constants that depend on the nature of the adsorbate and the adsorbent (24). Freundlich constant at equilibrium k_F indicates the adsorption capacity of each catalyst was as follows: CN-Fe> CN> CN-Cu.

The constant n is related to the accessibility of the adsorbate to the surface of the adsorbent, i.e. the probability that a dye molecule has access to an adsorption site. When n takes a value of 1, it implies that the adsorption surface is a homogeneous plane in contact with a solution whose concentration is the same at any point in the system. If the value of n is less than 1, it means that there are limitations in the adsorption depending upon the surface morphology of the catalyst (26). The three catalysts have values of n lower than 1, indicative of the heterogeneity of the surface morphology (27). It can be observed that for the CN-Fe the value of n is close to 1, which indicates that the surface of this catalyst is less heterogeneous when compared with the one of CN and CN-Cu. For this reason, the adsorption of DB1 on the surface of this catalyst was favoured. This can be because the adsorption occurs also on the preponderant and homogeneous sites of the exposed faces of nanoparticles of iron oxide (on this regard read the Supplementary Information).

3.2.3. Photocatalytic activity

Figure 4 shows the results of photocatalytic activity of the synthesized catalysts, the same that was evaluated for the degradation of the blue dye DB1 under the incidence of a Xe lamp.

Photo-degradation of the DB1 blue dye was also carried out, under the same conditions, in the absence of hydrogen peroxide, only with the catalyst, in the presence of the Xe lamp and no decrease in dye concentration was recorded. In this case, this was due to the absence of the

oxidizing agent since the photocatalytic decomposition of hydrogen peroxide allows the formation of hydroxyl radicals, necessary to carry out an AOP (28).

Table 2 shows the kinetic parameters calculated for the degradation tests of the DB1 blue dye. The four experiments responded to a pseudo-first order kinetics. It can be seen that when treating the dye only with the oxidizing agent, hydrogen peroxide, a degradation of 9.13% was achieved after 70 min of treatment, resulting in a kinetic constant of 0.018 min^{-1}. For the degradation of the DB1 blue dye in the presence of the catalysts, kinetics of 0.0939 min^{-1}, 0.0392 min^{-1}, and 0.117 min^{-1} were obtained for CN, CN-Cu, and CN-Fe, respectively. It was possible to degrade the dye in percentages greater than 99%. This percentage degradation was achieved after 50 min with CN, at 70 min with the CN-Cu, and for CN-Fe the time was 35 min. These results indicate that polymeric carbon nitride exhibits a considerable photocatalytic activity, further revealing that both catalyst and oxidizing agent are necessary for an efficient photodegradation reaction.

Doping the catalyst with metals is intended to enhance its photocatalytic activity. However, the degradation of the DB1 blue dye is not favoured by using copper-doped carbon nitride as a catalyst. This is because some of the electrons are captured by the Cu (I) and Cu (II) sites and oxidation and reduction cycles are generated [9]. Copper has been more effective as a selective and specific catalyst to oxidize aromatics alcohols to either aldehyde or carboxylic acids [9]. On the other hand, the use of iron doped carbon nitride improves the efficiency of the reaction with respect to pure carbon nitride. Generally, larger surface areas favour the photocatalytic activity since there more active sites are available.

Therefore, the result is due to a combination of a larger area, and a large amount of iron oxides nanoparticles deposited on the carbon nitride surface. Additionally, the electronic structure of iron-doped nitride also contributes significantly to its photocatalytic reactivity (7).

Table 3 shows the removal of TOC removal by conducting the degradation of the dye with each of the catalysts. The effectiveness in removal of TOC occurs in the following order: CN-Fe> CN> CN-Cu. Even though there is actually removal of chemical oxygen demand (COD), the TOC removal did not exceed the 15%.

3.3. Reuse of catalysts

One of the advantages of heterogeneous catalysis is that it is relatively easy to separate the catalyst from the rest of the system in order to be able to use it again. In this research, experiments were carried out to determine the feasibility of reusing carbon nitride-based catalysts up to three times.

The tests were performed under the same conditions mentioned for photo-degradation. The treatment time for the different catalysts was the time at which removals greater than 99% were achieved in previous tests: 50, 70 and 35 min for CN, CN-Cu, and CN-Fe, respectively.

The reuse results show that for the synthesized catalysts, the degradation of the DB1 dye remained above 99% during the three reuse cycles. That is, by using the same catalyst fraction up to three times, a removal of more than 99% is always ensured with the times determined for the first cycle. Similarly, (11) reported the feasibility of reusing pure and metal-doped carbon nitrides with a slight decrease in the photo-degradation capacity, which was attributed to the catalyst losses between one test and another. In our case, the experiments were carried out in such a way as to ensure that there were no losses between one degradation cycle and another

(according to the procedure described in section 2.3). In fact, experiments were performed in nine different Petri boxes. All catalyst samples were subjected to a first photo-degradation. Three samples were used in what was considered the first reuse, the samples were centrifuged and the residual concentration was measured. Three other samples were subjected to two more cycles of degradation, and the last three samples were used to degrade three times the dye before being subjected to centrifugation. This ensured that there were no losses in the process.

4. Conclusions

Pure polymeric carbon nitride (CN), polymeric carbon nitride doped with copper (CN-Cu), and a composite material of polymeric carbon nitride, amorphous carbon, and iron oxides (CN-Fe) were obtained with gravimetric yields of 2.38%, 5.88% and 2.10%, respectively. However, the content of the doping metal varied substantially: copper content was 0.585 wt% and iron was 37 wt%. Copper was mainly coordinated as Cu(I) and Cu(II) ions, while iron formed oxides of Fe(III). The adsorption equilibrium of the DB1 dye was reached at 10 min for pure carbon nitride and at 120 min for the catalysts doped with copper and iron. The percentages of removal of the DB1 dye by adsorption were 11.07%, 6.82% and 18.28% for CN, CN-Cu and CN-Fe, respectively. The adsorption of the blue dye DB1 with the catalysts responds to the Freundlich model. The best results of photocatalysis were obtained with CN-Fe which removed more than 99% of the dye (concentration of 500 mg L^{-1}, 10 mg of catalyst) in 35 min with a pseudo-first order kinetics with a constant 0.1107 min^{-1}. Although, the catalyst doping is intended to improve the photocatalytic properties, this is not the case with copper-doped carbon nitride, whose kinetic constant is 0.0392 min^{-1} versus a constant of 0.0939 min^{-1} for pure carbon nitride. The larger efficiency of the iron-doped catalyst is due to both higher surface area and

higher content of the co-catalyst. This new material was a composite of Fe(III) oxide nanoparticles (FeO(OH)), acting as a co-catalyst, wrapped in a matrix composed of carbon nitride and amorphous carbon with the potential to be used to several photo-oxidation reactions. It is feasible to reuse the catalysts without losing efficiency in the process in terms of treatment times or removal percentages. TOC removals of 11.34%, 2.86%, and 14.46% were achieved by using pure, copper-doped, and iron-doped carbon nitride, respectively.

REFERENCES

1. Mansor, N., Jorge, A., Brett, D., Gibbs, C., Corà, F., and McMillan, P. (2014). Graphitic carbon nitride supported catalysts for polymer electrolyte fuel cells. *J. Phys. Chem.*, 118: 6831--6838.

2. Thomas, A., Fischer, G., Antonietti, M., Muller, J., Schlogl, R., and Carlsson, J. (2008). Graphitic carbon nitride materials: variation of structure and morphology and their use as a metal-free catalysts. *J. Mater. Chem.*, 18: 4893--4908.

3. Xu, J., Wu, F., Wu, H., Xue, B., Li, Y., and Cao, Y., (2014). Three-dimensional ordered mesoporous carbon nitride with large mesopores: Synthesis and application towards base catalysis. Microposous and mesoporous materials, *Micropor. Mesopor. Mat.*, 198: 223--229.

4. Dante, R.C., Martin-Ramos, P., Correa-Guimaraes, A., and Martin-Gil, J. (2011). Synthesis of graphitic carbon nitride by reaction of melamine and uric acid. *Mater. Chem. Phys.*, 130: 1094--1102.

5. Liu, J., Zhang, T., Wang, Z., Dawson, G., and Chen, W. (2011). Simple pyrolysis of urea into graphitic carbon nitride with recyclable adsorption and photocatalytic activity. *J. Mater. Chem.*, 21: 14398--14401.

6. Rivera-Tapia, E. D., Fajardo, C.A., Ávila-Vega, Á.J., Ávila, C.F., Sánchez-Arévalo, F.M., Chango-Villacís, I., Javier Quiroz-Chávez, F., Santoyo-Salazar, J., and Dante, R.C. (2016) Synthesis of boron carbon nitride oxide (BCNO) from urea and boric acid, *Fuller. Nanotub. Car. N.*, 24: 8--12.

ACCEPTED MANUSCRIPT

7. Luo, J., Cui, Z., and Zang, G. (2013). Mesoporous metal-containing carbon nitrides for improved photocatalytic activities. *Journal of Chemistry*, Article ID 945348.

8. Han, H., Ding, G., Wu, T., Yang, D., Jiang, T., and Buxing, H. (2015). Cu and Boron doped carbon nitride for highly selective oxidation of toluene to nezaldehyde. *Molecules*, 20: 12686--12697.

9. Dante, R.C., Sánchez-Arévalo, F.M., Chamorro-Posada, P., Vázquez-Cabo, J., Huerta, L., Lartundo-Rojas, L., Santoyo-Salazar, J., Solorza-Feria, O., Diaz-Barrios, A., Zoltan, T., Vargas, F., Valenzuela, T., Muñoz-Bisesti, F., and Quiroz-Chávez, F.J. (2016) Fuller. Nanotub. Car. N. 24: 171--180.

10. Yuan, Q., Guan, B., Jin, S., Jun, H., and Xin, Y. (2016) Facile synthesis of carbon-doped graphitic C3N4@MnO2 with enhanced electrochemical performance. *RSC Adv.*, 6: 83209--83216.

11. Sridharan, K., Kuriakose, T., Philip, R., and Joo, T. (2014) Transition metal (Fe, Co and Ni) oxide nanoparticles grafted graphitic carbon nitrides as efficient optical limiters and recyclable photocatalysts. *Appl. Surf. Sci.*, 38: 139--147.

12. Tonda, S., Kumar, S., Kandula, S., and Shanker, V. (2014) Fe-doped and –mediated graphitic carbon nitride nanosheets for enhaced photocatalytic performance under natural sunlight. *J. Mater. Chem.* A, 2: 6772--6780.

13. Wang, Y., Wang, X. and Antonietti, M. (2012) Polymeric graphitic carbon nitride as a heterogeneous organocatalyst: from photochemistry to multipurpose catalysis to sustainable chemistry. *Angew. Chem. Int. Ed. Engl.*, 51: 68--89.

14. Lin, Q., Li, L., Liang, SS., Liu, M., Bi, M., and Wu, L. (2014) Efficient synthesis of monolayer carbon nitride 2D nanosheet with tunable concentration and enhanced visible – light photocatalytic activities. *Appl. Catal-B: Environ.,* 163: 135--142.

15. Yan, S., Li, Z., and Zou, Z. (2009). Photodegradation Performance of g-C3N4 Fabricates by Directly Heating Melamine. *Langmuir*, 25: 10937 – 10401.

16. Christie, R., Colour Chemistry, *The Royal Society of Chemistry (RSC Paperbacks)*, 1st Ed. 2001.

17. Puvaneswari, N., Muthukrishnan, J., and Gunasekaran, P. (2006) Toxicity assessment and microbial degradation of azo dyes. *Indian J. Exp. Biol.*, 44: 618 – 626.

18. Cesaro, A., Naddeo, V. and Belgiorno, V. (2013) Wastewater treatment by combination of advanced oxidation processes and conventional biological systems. *J. Bioremediat. Biodegrad.*, 4: 208--215.

19. Matsumoto, Y. (1996) Energy positions of oxide semiconductors and photocatalysis with iron complex oxides. *J. Solid State Chem.*,126: 227--234.

20. Maneerung, T., Liew, J., Dai, Y., Kawi. S., Chong, C. and Wang, C. (2016) Activated carbon derived from carbon residue from biomass gasification and its application for dye adsorption: Kinetics, isotherms and thermodynamic studies. *Bioresource Technol*., 200: 350–359.

21. Rivas, C., Nuñez, O., Longoria, F. and Gonzalez, L. (2014). Langmuir and Freundlich isotherms as model for the adsorption of nucleic acid components on WO3. *Saber,* 26: 43--49.

22. Djilani, C., Zaghdoudi, R., Djazi, F., Bouchekima, B., Lallam, A., Modarressi, A., and Rogalski, M. (2015). Adsorption of dyes on activated carbon prepared from apricot stones and commercial activated carbon. *J. Taiwan Inst. Chem. E.*, 53: 112--121.

23. Lee, S., Jun, Y., Lee, E., Heo, N., Hong, W., Huh, Y., and Chang, Y. (2015) Selective silver ion adsorption onto mesoporous graphitic carbon nitride. *Carbon*, 95: 58--64.

24. Vega, F., Covelo, E., and Andrade, M. (2011) Applying Freundlich, Langmuir and Temkin models in Cu and Pb soil sorption experiments. *Span. J. Soil Sci.*, 1: 20--37.

25. Haque, E., Jun, J., Talapaneni, S., Vinu, A., and Jhung, S. (2010) Superior adsorption capacity of mesoporous carbon nitride with basic CN framework for phenol. *J. Mater. Chem.*, 20: 10801- 10803.

26. Skopp, J. (2009) Derivation of the Freundlich adsorption isotherm from kinetics. *J. Chem. Educ.*, 86: 1 341--1343.

27. Lee, S., Jun, Y., Lee, E., Heo, N., Hong, W., Huh, Y., and Chang, Y. (2015) Selective silver ion adsorption onto mesoporous graphitic carbon nitride. *Carbon*, 95: 58--64.

28. Legrini, O., Oliveros E. and Braun, M. (1993) Photochemical process for water treatment. *Chem. Rev.*, 93: 671--698.

Table 1. Equilibrium adsorption, Langmuir's and Freundlich's parameters for CN, CN-Cu, and CN-Fe.

Assay	Parameter	Catalyst		
		CN	CN-Cu	CN-Fe
Adsorption equilibrium	C_e(mg/L)	444.63±6,14	465.90±1,03	408.60±2,73
	Time (min)	10	120	120
Langmuir	k_L (L/mg)	$-1,6 \cdot 10^{-03}$	$-1,5 \cdot 10^{-03}$	$-8,36 \cdot 10^{-05}$
	Q_{max} (mg g^{-1})	-22.9872	-13.5612	-2919.853
	R^2	0.9682	0.9610	0.1873
Freundlich	k_F (L mg^{-1})	$2.66 \cdot 10^{-09}$	$6,93 \cdot 10^{-10}$	0.2014
	n (mg g^{-1})	0.2564	0.2482	0.9636
	R^2	0.9859	0.9782	0.9942

Table 2. Kinetic parameters for the DB1 degradation with hydrogen peroxide (H_2O_2 alone, pure carbon nitride (CN), copper doped (CN-Cu) and iron doped (CN-Fe).

Catalyst	k (min^{-1})	R^2	Time (min) for 99% dye degradation
without catalyst	0.0018±0.0000407	0.9925	not determined by experiments
CN	0.0939±0.0011	0.9866	50
CN-Cu	0.0392±0.0028	0.9737	70
CN-Fe	0.1107±0.0065	0.9310	35

ACCEPTED MANUSCRIPT

Table 3. Removal of TOC for the tests carried out with pure polymeric carbon nitride CN, copper doped CN-Cu, and iron doped CN-Fe.

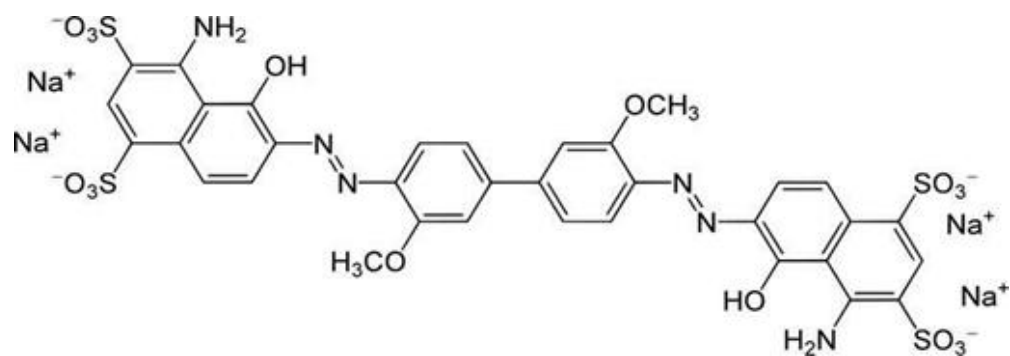| Catalyst	TOC (mg/L)	Removal (%)
without catalyst	84.90 ± 2,85	NA
CN	75.27 ± 2,60	11.34
CN-Cu	82.48 ± 0,87	2.86
CN-Fe	72.62 ± 2,45	14.46

Figure 1. Molecular structure of the deep blue DB1 dye.
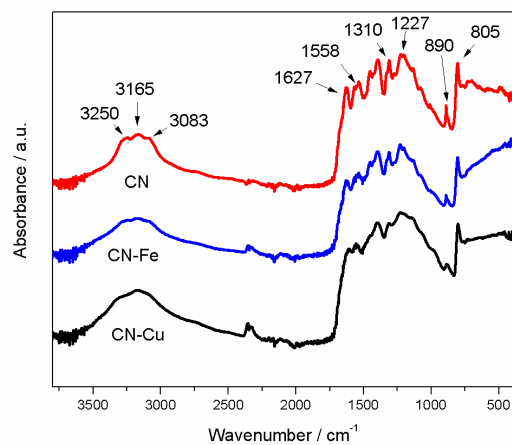
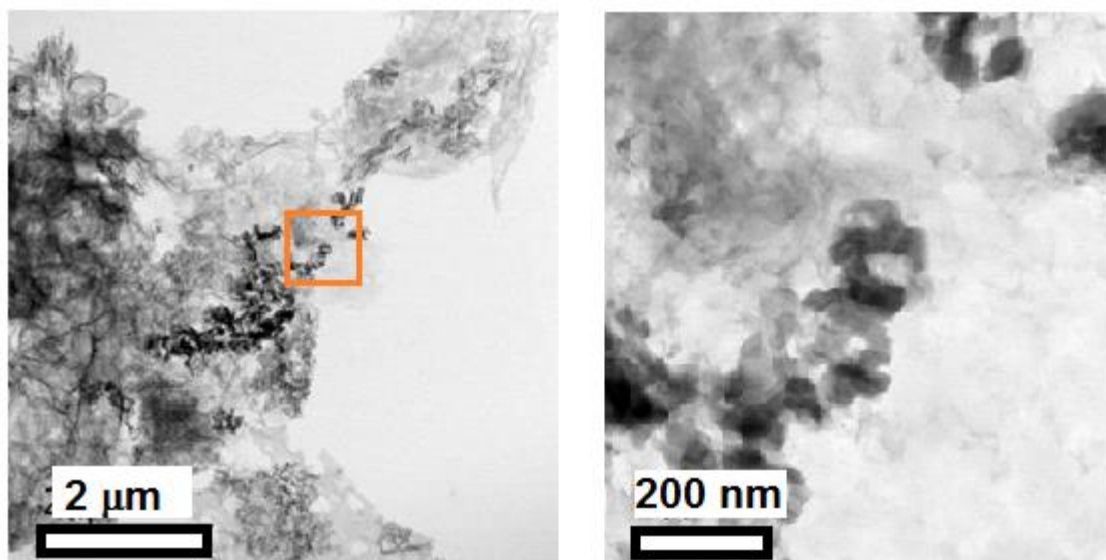**Figure 2.** Fourier transform spectra of the three samples: CN, CN-Fe, CN-Cu.

Figure 3. Left: TEM image of iron oxide particles (dark particles) wrapped in the composite matrix of carbon nitride and amorphous carbon. Right: TEM magnification of the box of the previous image, showing the details of a cluster of iron oxide nanoparticles embedded in the matrix.
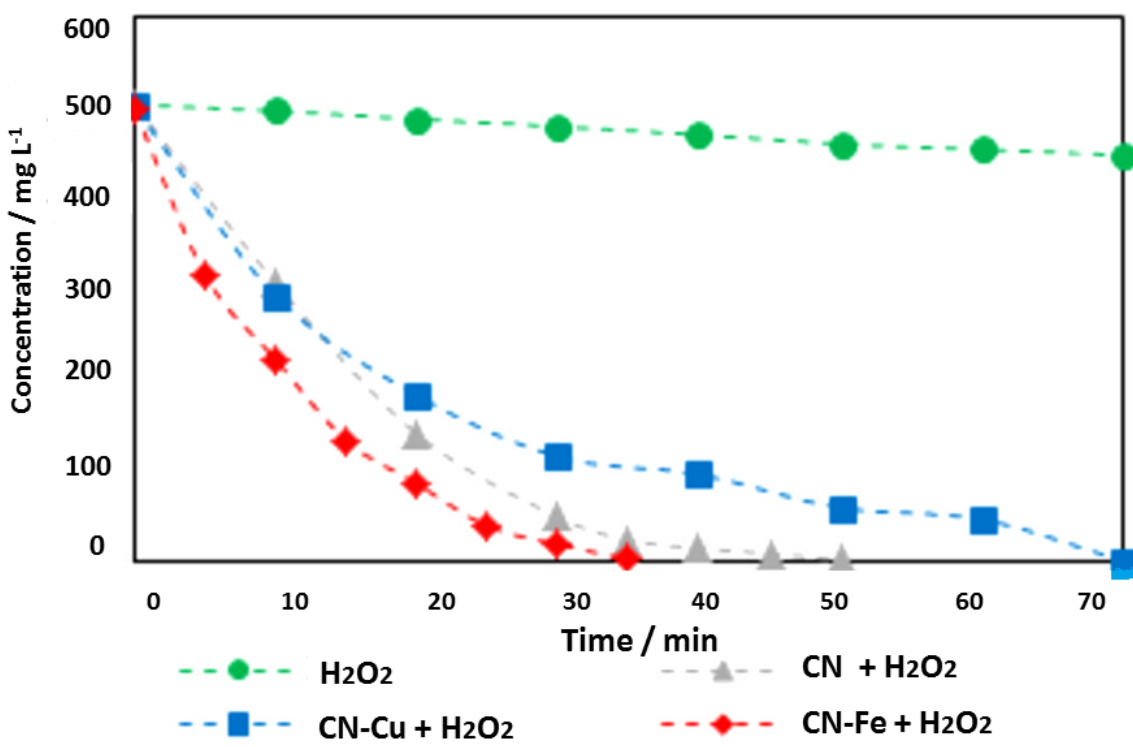
ACCEPTED MANUSCRIPT

Figure 4. Photocatalytic degradation of DB1 with H_2O_2 (1.43 V%, according to the method described in Section 2.2.3.) using the synthesized photo-catalysts: CN, CN-Cu, CN-Fe (20 mg of catalyst for 21 ml of solution, 500 ppm of DB1), and a solution of H_2O_2 (1.43 V%) alone as a reference.